

Frascati, December 16, 1996

Note: **MM-20**

**MEASUREMENTS ON TESLA SPLITTER PROTOTYPE
FOR THE DAΦNE MAIN RINGS**

*C. Biscari, B. Bolli, N. Ganlin, F. Iungo, F. Losciale, M. Paris,
M. Preger, C. Sanelli, F. Sardone, F. Sgamma, M. Troiani*

1. Introduction

The prototype of the Splitter Magnet, built by TESLA Engineering, Storrington (U.K.), was delivered to LNF on July 19, 1996. Due to summer holidays, the magnetic measurements and magnet characterization started beginning of September and took about two weeks. The measurements confirmed the design goals and the good quality of the construction. In fact, there has not been any necessity of magnetic length adjustment, that means no machining of the pole end caps. The other three splitter magnets will be delivered before the end of the year.

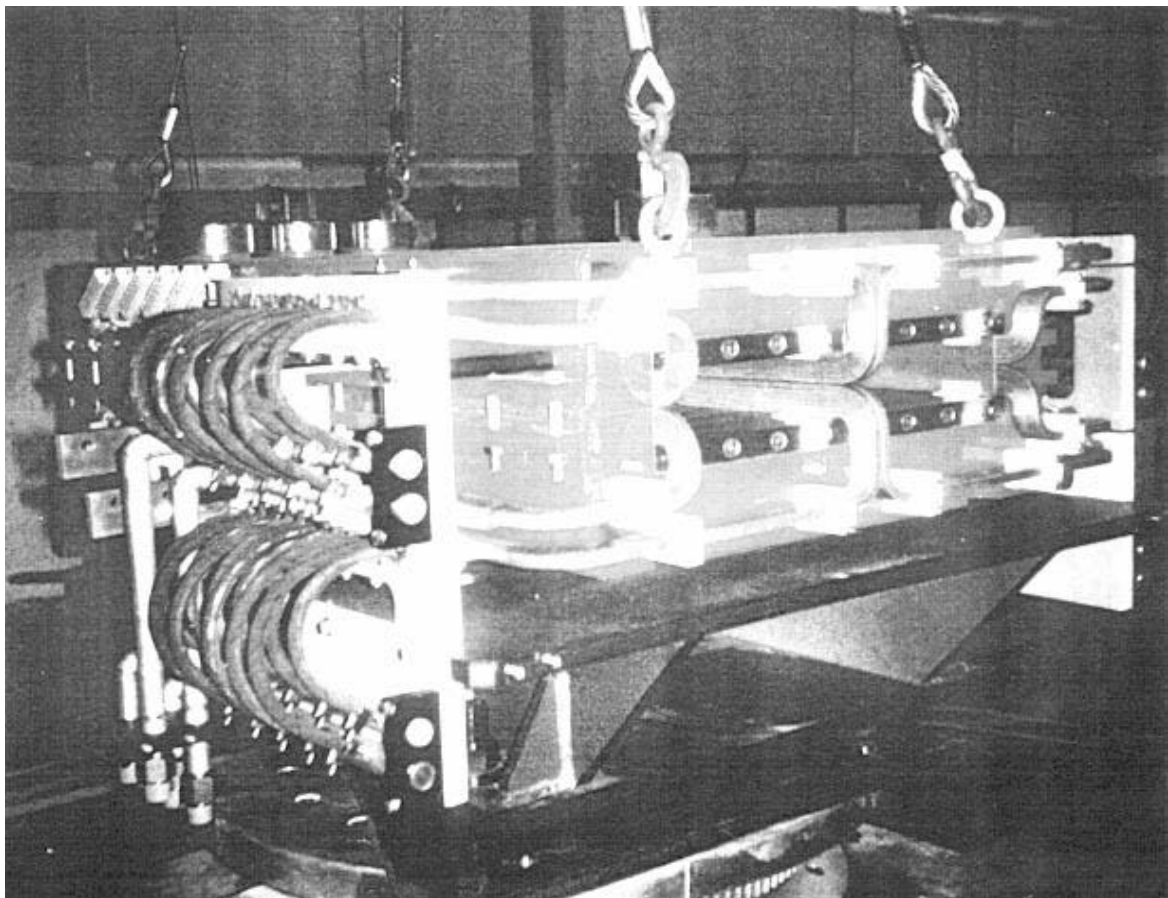


Figure 1 - The Splitter magnet on the magnetic measurement bench.

The magnet, shown in Fig.1, was designed by LNF staff. Table I gives its main parameters.

TABLE I - Splitter magnet prototype parameters.

Energy	MeV	510	750
Coil current	A	436.0	641.3
Measured field at magnet center	G	1768	2696
Deflection Angle	deg	8.75	8.75
Magnetic Length (Design)	mm	1450	1450
Measured length (B/B _C)dl	mm	1469.5	1471.9
Magnet gap	mm	75.3	75.3
Number of coils		4	4
Number of turns per coil		12	12
Copper conductor cross section	mm*mm	5.6 * 5.6	5.6 * 5.6
Cooling hole diameter	mm	3.6	3.6
Independent power supplies		2	2

2. Electrical measurements

The resistance of the splitter magnet coils was measured by means of a micro-ohm-meter (AOIP mod. OM 20) at room temperature. Looking at the magnet from the side where the three alignment sockets are mounted, we can define a Left and a Right side. The measured value was:

$$R_{\text{Left}} = 93.4 \text{ m} \quad @ 23 \text{ }^{\circ}\text{C}$$

$$R_{\text{Right}} = 93.6 \text{ m} \quad @ 23 \text{ }^{\circ}\text{C}$$

The same measurement was accomplished by using the Volt-Ampere method and the following data was measured:

$$V_{\text{Left}} = 40.4 \text{ V} @ 440.4 \text{ A, corresponding to } 92 \text{ m}$$

$$V_{\text{Right}} = 40.5 \text{ V} @ 440.4 \text{ A, corresponding to } 92 \text{ m}$$

These values were obtained at the same room temperature as in the preceding measurement. The agreement between the results obtained with the two different methods is very good.

The inductance and resistance of each half of the magnet prototype were also measured by means of a LCR meter (LCR meter HP 4284 A) at different frequencies. The results are very similar and they are shown in Figure 2. The corresponding dc values can be extrapolated from these data. They are consistent with the measured and design data.

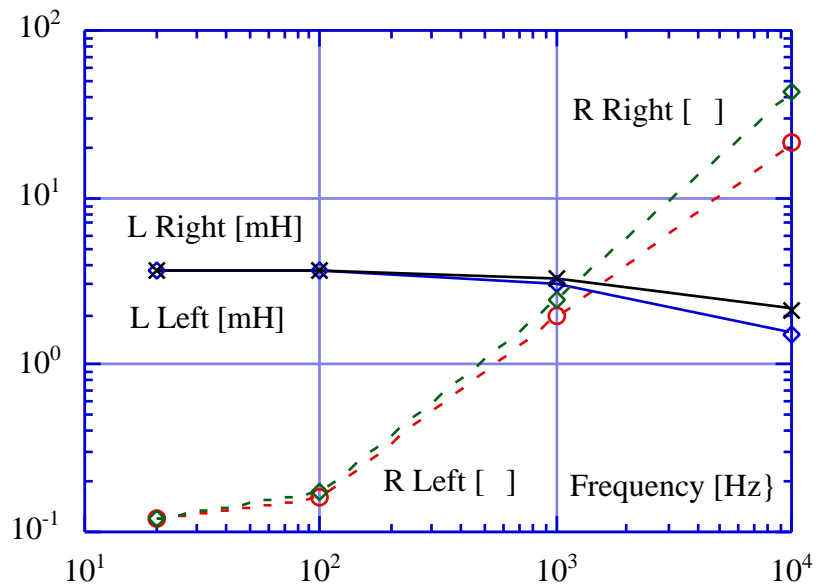


Figure 2 - Resistance and inductance versus frequency for the Splitter Magnet

Thermal measurements were also accomplished and the worst figure for the Splitter magnet is listed in Table II.

TABLE II - Temperature rise of magnet coils.

Time (min)	0	3	6	9	12
Temperature (°C)	25.1	27.9	27.9	28.0	28.2

3. Magnetic measurements

Due to the length of the iron yoke (1380 mm), it was not possible to measure the whole magnet with a single scan of the Y axis of the computer controlled Hall probe positioning system of the magnetic measurements laboratory [1]. The magnet has therefore been placed on the rotating support used for the Accumulator dipole measurements [2], adapted to perform a 180° rotation around its vertical axis. The splitter has been carefully aligned by measuring the coordinates of the Taylor Hobson alignment spheres on top of the magnet in both the "normal" and "reverse" positions of the rotating support. The magnet is in the "normal" position, when the Hall probe enters the gap from the side with one Taylor-Hobson sphere (see Fig.1): when installed in the Main Rings, this is the side looking at the interaction point. On the other side, the "reverse" one, there are three alignment spheres which, together with the single sphere on the other side, give the directions of the two ring arcs after the splitter.

However, even with this arrangement, the longitudinal extension of the field, including the fringing contributions, is such that it cannot be completely covered by Hall probe positioning system. It was therefore decided to measure the field in the fringing, leaving a 32 cm region around the magnet center unmeasured. As shown in the following, the field in this region is very flat, and can be easily interpolated.

Although in its final configuration in the Main Rings the right and left coils will be powered by two independent power supplies, only one, capable of reaching the maximum current, was available in the laboratory to carry out the measurement of the splitter field. The coils were therefore connected in series. Figure 3 shows the field in the right gap (which drives the beam into the short arc), measured at the inner position allowed by the positioning system, 16 cm from the center in the longitudinal direction, at the center of the gap in the transverse one, versus the excitation current with the right and left coils in series. Figure 4 shows the difference between the fields measured in the right and left gaps at the same excitation current, which can be fitted accurately with a second order polynomial. The relative difference reaches a maximum value of 2.5‰ at full current.

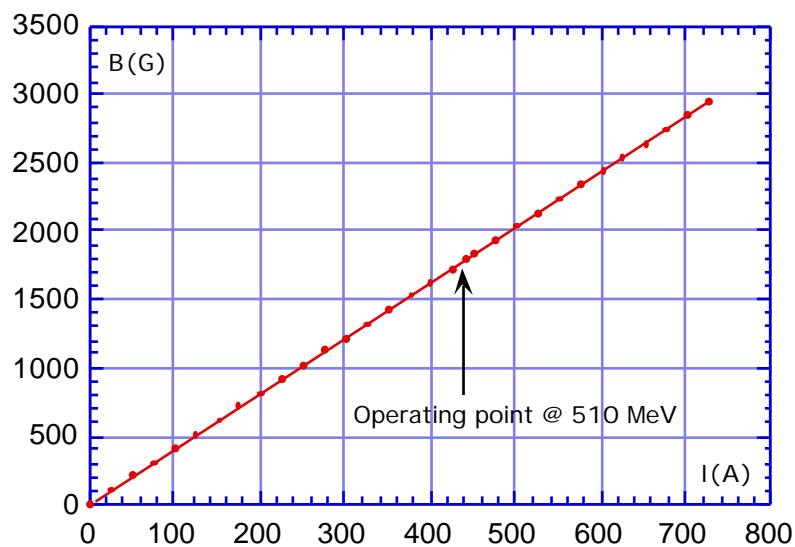


Figure 3 - Vertical field component in the right gap versus current.

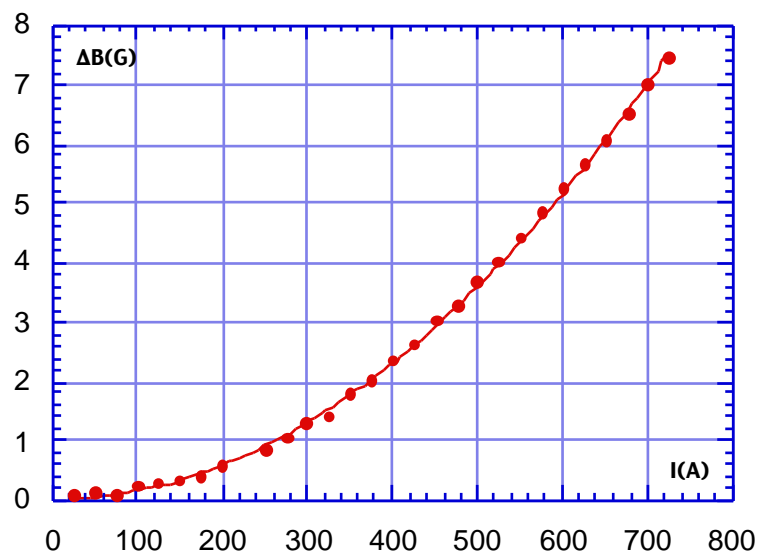


Figure 4 - Difference between the fields in the right and left gap versus current.

The splitter is equipped with removable end caps to adjust the magnetic length to the desired value. It is a rather complicated task to give a good definition of the magnetic length for the splitter magnet, where the beam enters at an angle and a position which depend on the crossing angle of the beams at the interaction point. The trajectory inside the magnet and the exit point and angle depend on the crossing angle as well. Figure 5 shows the nominal trajectory in the splitter, in the rectangular field approximation, together with the size of the splitter gaps.

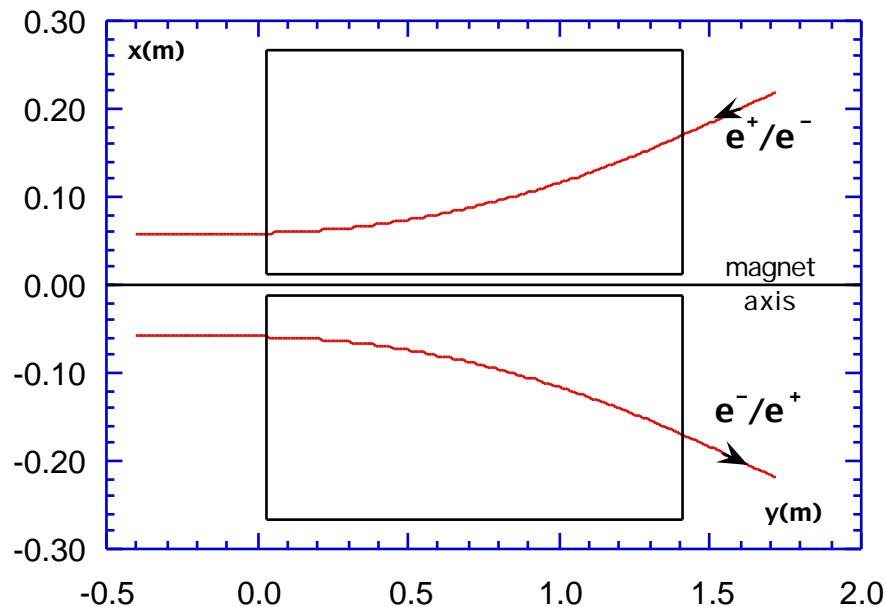


Figure 5 - Nominal beam trajectory in the splitter. The rectangles show the free aperture in the gaps between the coils.

A reasonable method of determining the optimum iron length is to measure the field in the whole magnet, track a particle with the initial conditions corresponding to the nominal working point (± 12.5 mrad at the crossing point), find the particle energy at which the trajectory is bent by the correct bending angle (8.75°) and check the distance of the output trajectory from that calculated in the rectangular model approximation for the splitter magnet (see Figure 5).

We have therefore mapped the vertical field component along the whole span available to the Hall probe positioning system in steps of 10 mm both in the longitudinal and transverse directions. For each of the four maps (normal right, normal left, reverse right and reverse left) we have performed 20 longitudinal scans at different horizontal positions, beginning at 40 mm from the magnet symmetry axis and ending up at 230 mm from it. The boundaries are set by the size of the coils and Hall probe support. Each longitudinal scan consists of 100 points, starting at 43 cm from the ideal magnet edge (corresponding to the field step of the rectangular model) in order to measure the fringing field completely. The complete map consists therefore of 16000 measured points, and it has been performed at two excitation currents (440.38A and 652.57A).

Figure 6 shows the vertical field component along a straight line parallel to the magnet axis at a horizontal distance of 10 cm from it. The gap between the right and left sides of the plot corresponds to the points which were not measured because of the limited span of the Hall probe positioning system. Figure 7 is an expanded view of the central part of the magnet showing the amount of the approximation made in interpolating the unmeasured region as the average of the two measured points at its boundary. It can be noticed that the field variation in the flat top region is less than 1 G, thus well justifying the above mentioned approximation.

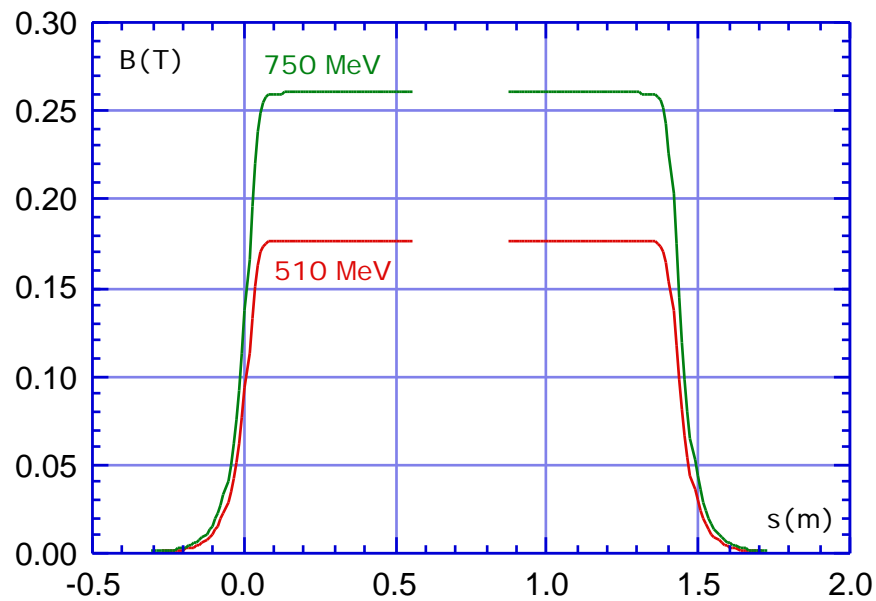


Figure 6 - Vertical field component along a straight line parallel to the magnet axis.

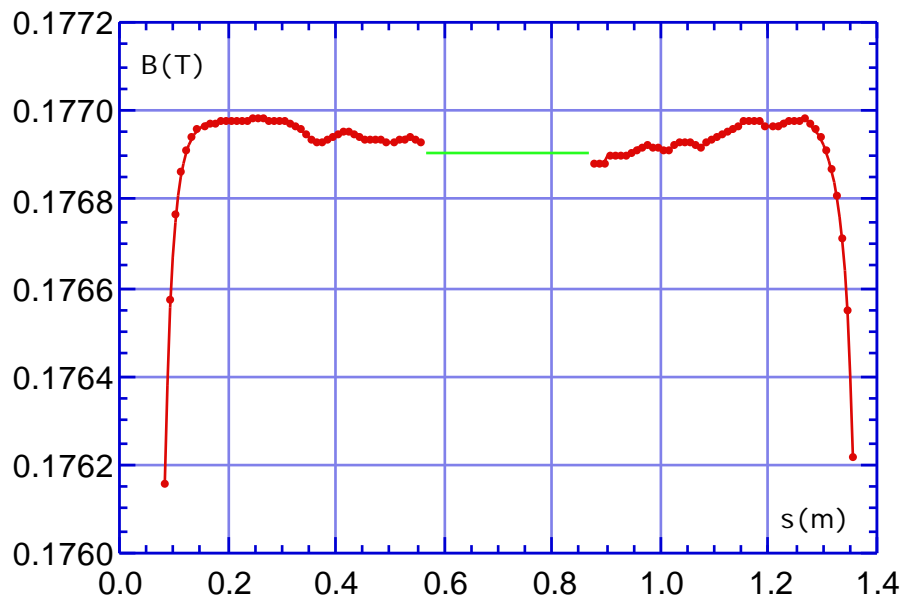


Figure 7 - Expanded view of the flat top region. The straight line in the center corresponds to the approximation performed in the unmeasured region (expanded scale).

The field at the inner measured point inside the gap is shown in Figure 8 as a function of the horizontal position. The first measured point is at ± 40 mm from the magnet axis because of the Hall probe support transverse size, and it is rather near to the entry point of the particles at their nominal trajectory (58.75 mm). The last one, at 230 mm from the axis, is well beyond the exit point of the trajectory (175.56 mm, see Figure 5). The field inside the magnet is remarkably constant: the variation is only 1 G on the whole measured aperture, in spite of the fact that it changes direction from one gap to the other one. The error bars are the sensitivity of the Hall probe measuring system.

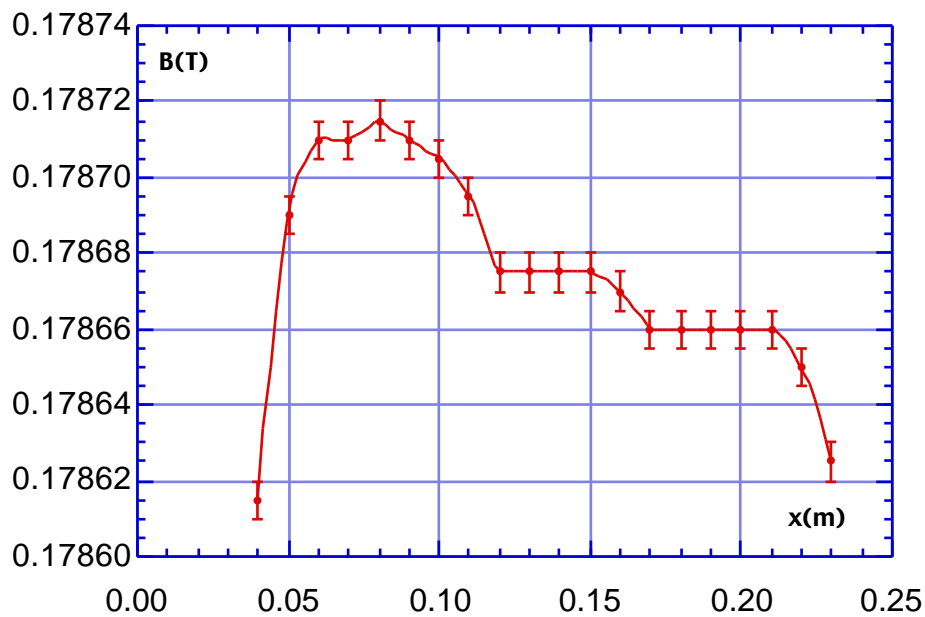


Figure 8 - Vertical field component at inner measured point versus horizontal position (expanded scale)

The dependence of the field on the horizontal position in the fringing field region is given in Figure 9. The longitudinal position of the horizontal scan corresponds roughly to the input boundary of the nominal magnet in the rectangular approximation. In this case (the scale is much wider than in Figure 8), being the nominal trajectory at 6 cm from the magnet axis, the beam feels a transverse gradient. The field is almost flat on the output side, where the beam passes at 18 cm.

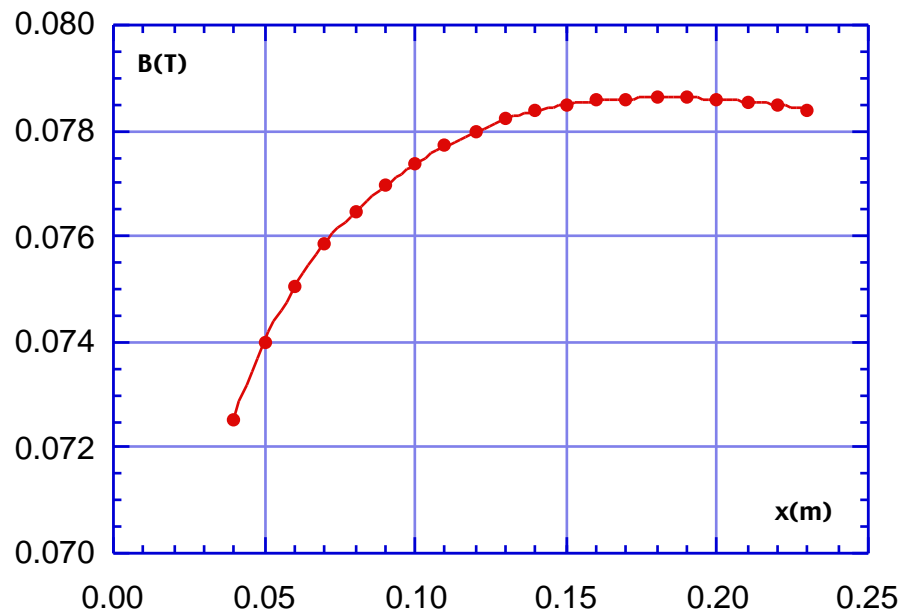


Figure 9 - Vertical field component near the edge of the ideal magnet ($y = -4.5$ mm) (expanded scale)

We have also checked the influence of one coil on the other gap by powering only the coil on the left side of the splitter and measuring the field in the right gap. Figure 10 shows the result of this measurement: as expected, there is a non negligible effect, of the order of 2%, only near the end cap on the inner side of the gap. Inside the iron yoke the contribution does not depend on the horizontal distance from the magnet axis and is of the order of 0.1%.

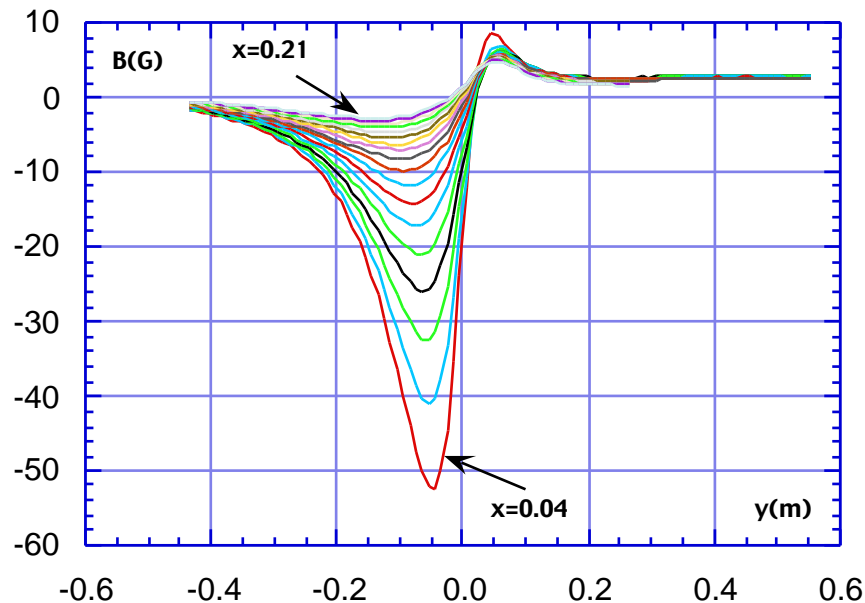


Figure 10 - Vertical field component in the right gap with only the left coil powered at 440.38A. The curves show the field along straight lines parallel to the magnet axis in steps of 10 mm.

In order to track the particle trajectory through the real field, we have used a parabolic interpolation method between the measured points. The result is shown in Figure 11, where the distance between the tracked trajectory and nominal one is plotted versus the longitudinal position along the symmetry axis of the splitter. On the same plot we show the result for the field maps measured on the right and left gaps, and for the two excitation currents (440.38A and 652.57A). The beam energy is used as a free parameter in the tracking to match the nominal angle between the input and output directions of the beam trajectory.

For this reason we find a slight difference in energy between the right and left gap at the same excitation current, due to the above mentioned small field difference between the two gaps (see Figure 4). This difference will be corrected in the collider by setting the independent power supplies at the correct current for each gap. As Figure 11 clearly shows, the four trajectories differ from each other by less than 0.1 mm. The offset of the output trajectory from the ideal one is $0.3 \div 0.4$ mm, which can be easily corrected by means of the "C" corrector [3] downstream the splitter in the beam path. We have verified, by simulating a shorter or longer iron yoke, that the offset is mainly due to the asymmetry of the field in the longitudinal direction, which cannot be corrected easily by changing the thickness of the removable end caps. We have therefore decided to leave the total iron length unchanged with respect to the original design.

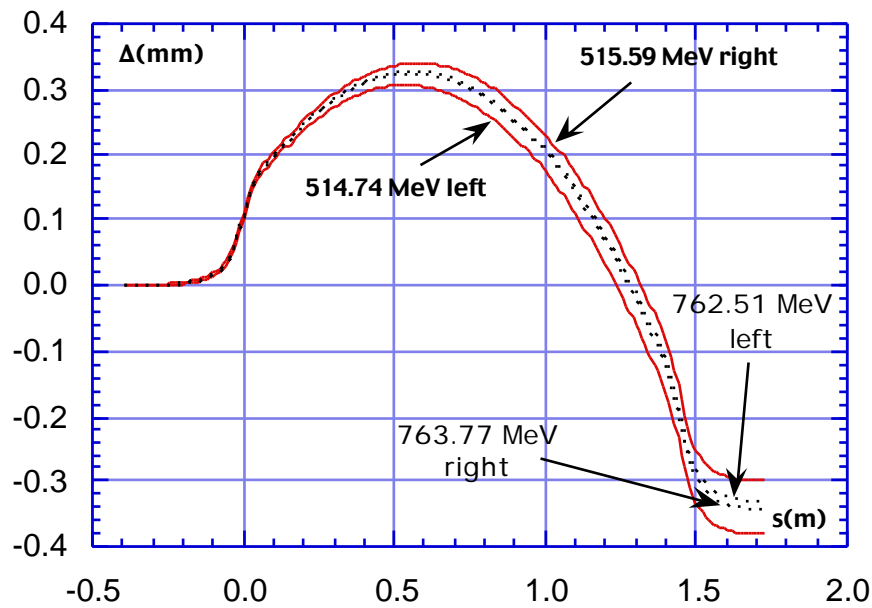


Figure 11 - Displacement of the calculated beam trajectory from the nominal one.

By using the same interpolation method between the measured points, it is possible to expand the field in a power series around the nominal trajectory, as previously done in the analysis performed on the Accumulator and Main Rings bending magnets [4,5], to find the amount of high order contributions in the field, which may affect the beam dynamics. Figure 12 shows the first order term of the transverse expansion at the nominal operating energy. The peak at the magnet input is due to the transverse gradient near the inner coil in the fringing field region (see Figure 9), while the peak at the output is due to the angle between the iron yoke and the beam trajectory (9° , see Figure 5).

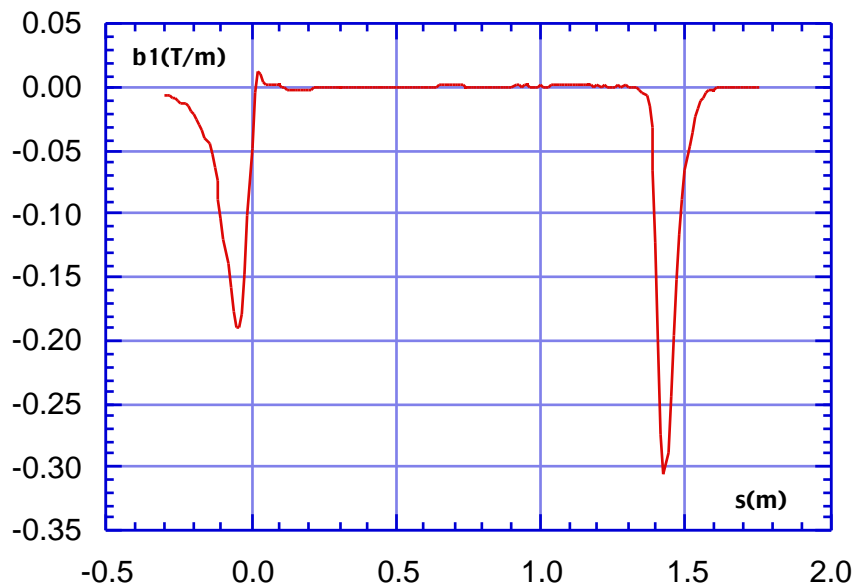


Figure 12 - First order term of the field transverse expansion around the nominal trajectory.

Figures 13, 14 and 15 show, respectively, the second, third and fourth order terms of the transverse expansion. In these three graphs the contribution of the input fringe is always much larger than the output one: this is due to the proximity of the trajectory to the coil at the splitter input, while at the output the beam passes in the region where the field is almost flat (18 cm from the magnet axis, see Figure 9). Table III gives the integrated contributions of the high order terms.

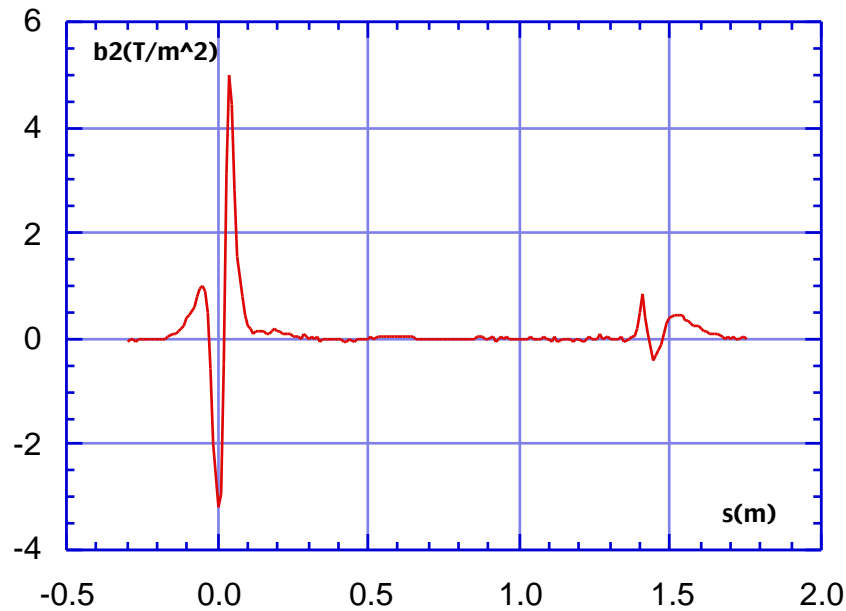


Figure 13 - Second order term of the field transverse expansion around the nominal trajectory.

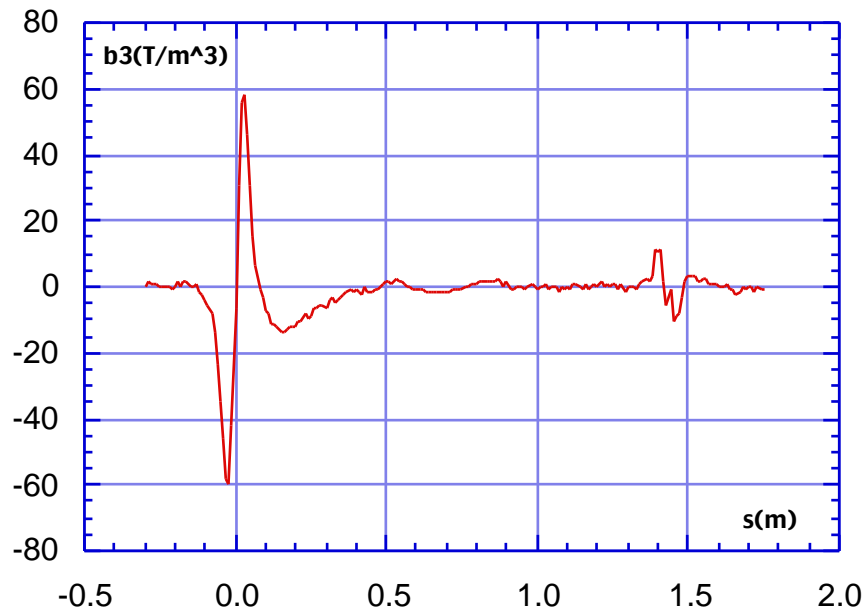


Figure 14 - Third order term of the field transverse expansion around the nominal trajectory.

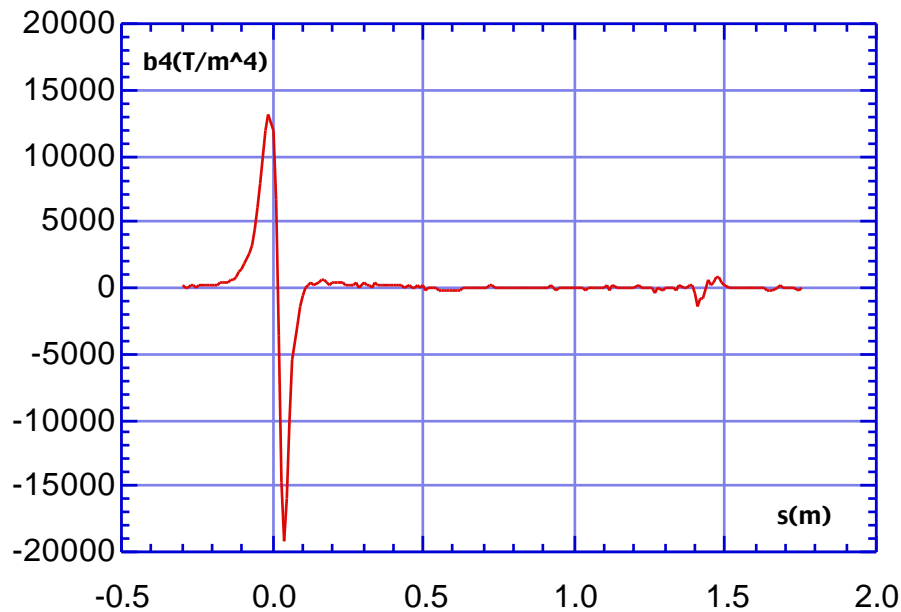


Figure 15 - Fourth order term of the field transverse expansion around the nominal trajectory.

TABLE III - Integrated high order terms

	440.38A	652.57A
$b_0 \cdot ds$ (T.m)	-.262	-.388
$b_1 \cdot ds$ (T)	-.044	-.065
$b_2 \cdot ds$ (T/m)	.236	.424
$b_3 \cdot ds$ (T/m ²)	-2.7	-4.9
$b_4 \cdot ds$ (T/m ³)	222	996

4. Conclusions

The results of the measurements have confirmed the validity of both the magnetic calculations and mechanical design, performed at LNF, and the very accurate job performed by TESLA Eng. in the realization of such a peculiar magnet. No modification of any kind was needed and Tesla has been authorized to the series production in a very short time. The Splitter prototype has now been installed in the DA NE hall and the other three splitter magnets are expected to be delivered at the end of this year, to be measured and installed at the beginning of 1997.

References

- [1] F. Iungo, M. Modena, Q. Qiao, C. Sanelli "DA NE Magnetic Measurement Systems" DA NE Technical Note MM-1 (4/11/1993).
- [2] A. Battisti, B. Bolli, F. Iungo, F. Losciale, M. Paris, M. Preger, C. Sanelli, F. Sardone, F. Sgamma, M. Troiani, S. Vescovi "Measurements and tuning of DA NE Accumulator dipoles" - DA NE Technical Note MM-9 (29/8/1995).
- [3] B. Bolli, N. Ganlin, F. Iungo, M. Modena, F. Losciale, M. Paris, M. Preger, C. Sanelli, F. Sardone, F. Sgamma, M. Troiani "Measurements on TESLA "C" corrector for the DA NE Main Rings" - DA NE Technical Note MM-17 (28/6/1996).
- [4] A. Battisti, B. Bolli, F. Iungo, F. Losciale, M. Paris, M. Preger, C. Sanelli, F. Sardone, F. Sgamma, M. Troiani, S. Vescovi "Measurements and tuning of DA NE Accumulator dipoles" - DA NE Technical Note MM-9 (29/8/1995).
- [5] B. Bolli, N. Ganlin, F. Iungo, F. Losciale, M. Modena, M. Paris, M. Preger, C. Sanelli, F. Sardone, F. Sgamma, M. Troiani "The "short" dipoles of the DA NE Main Ring achromats" DA NE Technical Note MM-19 (2/8/1996).